Electronic Supplementary Information

TPAOH assisted size-tunable Gd_2O_3@mSi core-shell nanostructures for multifunctional biomedical applications

E. Pavitra,[a,b] G. Seeta Rama Raju,[c] Ganji Purnachandra Nagaraju,[d] Goli Nagaraju,[b] Young-Kyu Han,[c] Yun Suk Huh,[a,] Jae Su Yu[b,]**

[a]*Department of Biological Engineering, Biohybrid Systems Research Center (BSRC), Inha University, Incheon, 402-751, Republic of Korea*

[b]*Department of Electronic Engineering, Kyung Hee University, 1 Seocheon-dong, Giheung-gu, Yongin-si, Gyenggi-do-446701, Republic of Korea*

[c]*Department of Energy and Materials Engineering, Dongguk University, Seoul 04620, Republic of Korea*

[d]*Department of Hematology and Medical Oncology, Winship Cancer Institue, Emory University, Atlanta, USA*

**E-mail:* yunsuk.huh@inha.ac.kr (Prof. Y. S. Huh) *jsyu@khu.ac.kr (Prof. J. S. Yu)*

Experimental section

Synthesis of $Gd_2O(CO_3)_2.H_2O:Eu^{3+}$ nanoparticles

$Gd_{2(1-0.05)}O(CO_3)_2 \cdot H_2O:Eu^{3+}$ (GdC) (herein, 5 mol% Eu^{3+}) nanoparticles with different sizes were prepared using a modified urea-based homogeneous precipitation method. All the chemical reagents used in these experiments were of analytical grade (from Sigma-Aldrich) and used as received. The solution was prepared by dissolving (1-x) mol of high-purity grade gadolinium nitrate hexahydrate [$Gd(NO_3)_3.6H_2O$], and x mol of europium nitrate pentahydrate [$Eu(NO_3)_3.5H_2O$] in 100 ml of de-ionized (DI) water. The solution was stirred vigorously using a magnetic stirrer and 3 g (30 mg/ml) of urea [NH_2CONH_2] was then added to the solution. After 2 h of continuous stirring, the required amount of TPAOH [$(CH_3CH_2CH_2)_4 \cdot N(OH)$]] was added to the solution and stirred until the formation of a homogeneous solution. The solution was then kept in a silicone oil-bath and the solution temperature was maintained at 90 ºC for 10 h. The reaction was repeated for different concentrations of TPAOH to examine the size tunability of the resulting nanoparticles. After gradually cooling the mixture to room temperature, the precipitate was separated from the colloidal solution using a centrifugal separator at 5000 rpm for 5 min and washed several times using ethanol and DI water. The precursor was then dried at 60 ºC for one day in an ambient atmosphere.

Synthesis of GdC@mSi core-shell nanoparticles

GdC@mSi CSNSs and CSNPs were prepared by a facile synthesis. Initially, 100 mg of GdC nanoparticles were dispersed in 15 ml of ethanol and ultrasonicated for 30 min. The sonicated solution was transferred to a 100 ml beaker containing 40 ml of DI water and 15 ml of ethanol, and stirred at room temperature for 30 min. The solution was mixed with 160 mg of hexadecyltrimethylammonium bromide (CTAB) with continuous stirring. After the

formation of a homogeneous solution, 0.6 ml of the ammonium hydroxide solution (NH_4OH) was added dropwise and the mixture was heated to 60 ºC on a hot plate and maintained for 30 min with continuous stirring. A mixture of 210 µl of tetraethyl orthosilicate [TEOS, $Si(OC_2H_5)_4$] and 10 ml of (3-aminopropyl)triethoxysilane (APTES) was added and after a few more minutes of stirring, 60 µl of 3-(trihydroxysilyl) propyl methyl-phosphonate, monosodium salt solution (3-THSPMP) was added drop wise. Magnetic stirring was continued at the same temperature for 3 h. The resulting GdC@mSi nanoparticles were separated using a centrifugal separator at 5000 rpm for 5 min and washed several times with ethanol to remove the unreacted species. The final product was re-dispersed in 50 ml of ethanol. Subsequently, 300 mg of ammonium nitrate (NH_4NO_3) was added to the above solution. To remove the CTAB template from CSNSs and CSNPs, the solution was allowed to heat up to 70 ºC for 1 h. Finally, the mesoporous CSNSs and CSNPs were collected by centrifugation, washed several times with ethanol and water. The resulting nanoparticles were dried in a vacuum desiccator. To obtain the Gd@mSi nanoparticles, the GdC@mSi CSNSs and CSNPs were calcined at different temperatures.

Synthesis of GdC@mSi@FA and Gd@mSi@FA core-shell nanoparticles

The as-prepared mesoporous GdC@mSi or Gd@mSi CSNSs and CSNPs were washed with dimethyl sulfoxide (DMSO) and 60 mg of GdC@mSi or Gd@mSi CSNSs and CSNPs were then re-suspended in a beaker containing 10 ml of DMSO and 10 ml of toluene. The solution was stirred at room temperature until the formation of a homogeneous solution. In another beaker, 30 mg of FA and 0.25 µl of APTES were dissolved in 10 ml of DMSO under ultra-sonication for 10 min. Subsequently, 0.35 mg of N-hydroxysuccinimide and 0.45 mg of 1-(3-dimethylaminopropyl)-3-ethylcarbodiimide hydrochloride were added to the above solution under continuous stirring for 2 h. The two solutions were then mixed and the reaction was held for 20 h under continuous magnetic stirring at room temperature. The nanoparticles

were collected by centrifugation washed twice with toluene and dried under vacuum.

Cell culture and cell proliferation

The U2OS cell line, which was originally known as the 2T line, was cultivated from the bone of a fifteen-year-old human female suffering from an osteosarcoma. The U2OS cell line was obtained from the American Type Culture Collection (ATCC, Manassas, VA). Characterization and authentication were reported by the ATCC in the accompanying certificate of analysis. The ATCC validated the cultures to be mycoplasma-free, expressed only basal epithelial cell markers and unique human DNA profile. They were then cultured in McCoy's 5A medium containing 1.5 mM L-glutamine and 2200 mg/L sodium bicarbonate (Cat # ATCC® 30-2007™ , ATCC, Manassas, VA) supplemented with 10% fetal bovine serum (Cat # 4135; Sigma-Aldrich, St. Louis, MO), 50 units/ml penicillin, and 50 µg/ml streptomycin (Life Technologies, Inc., Frederick, MD). The cells were incubated at 37 ℃ in a humidified atmosphere containing 5% CO_2.

In vitro fluorescence microscopy of GdC@mSi@FA nanoparticles uptake

In vitro cell nucleo-cytochemical analyses were performed as described earlier (Sun et al., 2010). For in vitro fluorescence microscopy of the nano particles uptake, U2OS cells were grown in 8 well chamber slides and treated with the nano-particles product for 18 h. The cells were fixed in 4% paraformaldehyde followed by washing three times with 1XPBS for 5 min. Subsequently, 4'-6-diamidino-2-phenylindole (DAPI) was used for nuclear counterstaining. The cells were then mounted and examined by fluorescence microscopy using a Zeiss LSM 510 Meta Confocal fluorescence microscope (Peabody, MA) equipped with laser lines of 405, 458, 477, 488, 514, 543, and 633 nm for excitation, emission and appropriate band pass filters

for collecting the DAPI, and nanoparticles emission signals.

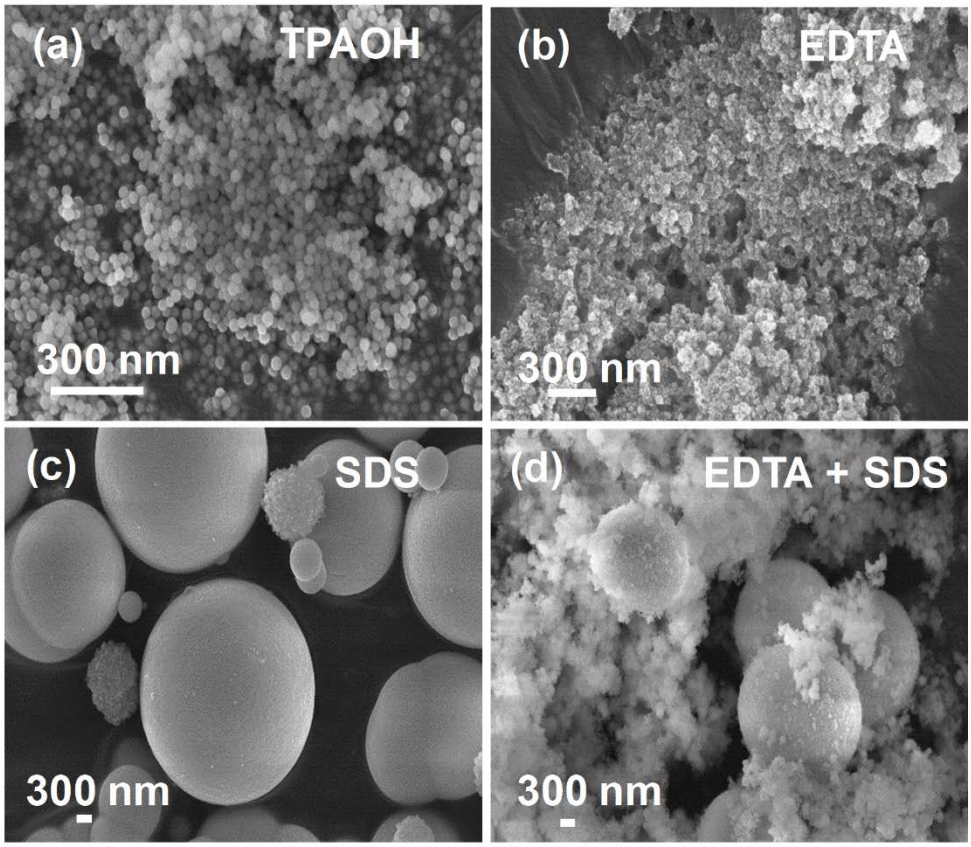

Fig. S1 GdC spheres synthesized with different surfactants: (a) Tetrapropylammonium hydroxide (TPAOH), (b) Ethylenediaminetetraacetic acid (EDTA), and (c) Sodium dodecyl sulfate (SDS).

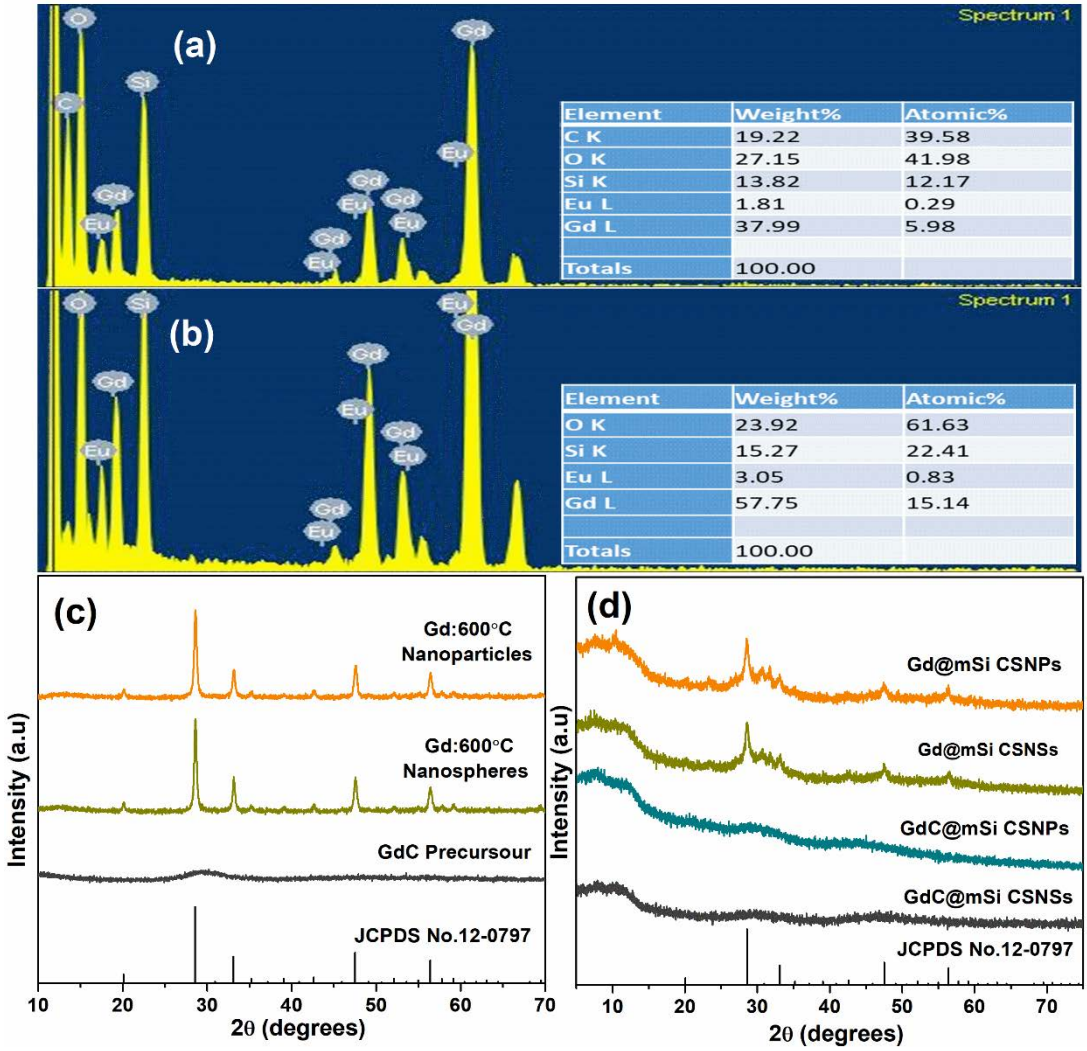

Fig. S2 (a) and (b) EDS spectra of GdC@mSi and Gd@mSi CSNSs and CSNPs. (c) XRD patterns of the GdC nanospheres and nanoparticles before and after calcination. (d) XRD patterns of the Gd@mSi CSNSs and CSNPs before and after calcination at 600 ºC.

The XRD patterns of the as-prepared precursor sample and calcined samples were presented in Fig. S2c. A broad band without a diffraction peak was noticed for the precursor sample, indicating an amorphous structure. The amorphous nature was attributed to the surface coating of organic impurities, such as CO_2, NH_4^+ and TPA^+. When the sample was calcined at 600 ºC, a well-crystallized Gd_2O_3:Eu^{3+} cubic phase was identified and all the XRD peaks were in good agreement with the standard JCPDS No. 12-0797 with the space group 1a-3. Fig. S2d displays the XRD patterns of the Gd@mSi core-shell CSNSs and CSNPs before and after

calcination at 600 ºC, which exhibited a similar trend to the bare Gd nanostructures. The XRD pattern of the precursors shows a broad amorphous silica peak at 2θ values between 5 and 15º; and two broad bands at 30º and 45º indicates the amorphous nature of the GdC@mSi samples. After calcining at 600 ºC, however, a cubic phase was obtained with some amorphous silica peaks and the intensity of the XRD pattern decreased when compared to the pure Gd_2O_3:Eu^{3+} samples.

PL Properties

The PLE spectra (insets of Fig.3) revealed a charge transfer band (CTB) with a band maximum at 258 nm overlapped with the f-f transition ($^8S_{7/2}\rightarrow{}^6I_{9/2}$) of Gd^{3+} ions at 277 nm in the higher energy region. The PLE spectra also consisted of narrow excitation bands due to the f-f transitions of Gd^{3+} and Eu^{3+} ions in the lower energy region, which were assigned to the electronic transitions ($^8S_{7/2}\rightarrow{}^6P_{7/2}$) at 315 nm, and ($^7F_0\rightarrow{}^5D_4$) at 361 nm, ($^7F_0\rightarrow{}^5G_4$) at 381 nm, ($^7F_0\rightarrow{}^5L_6$) at 393 nm, ($^7F_0\rightarrow{}^5D_3$) at 414 nm, ($^7F_0\rightarrow{}^5D_2$) at 465 nm and ($^7F_0\rightarrow{}^5D_1$) at 533 nm. A comparison of the GdC@mSi core-shell PLE (inset of Fig. 3(a & c)) with that of the Gd@mSi core-shell excitation (inset of Fig.3(b & d)) revealed a weak CTB and intense f-f transitions for the GdC@mSi samples, while strong CTB with low intense f-f transitions were observed for the Gd@mSi samples. This might be explained by the amorphous nature of the precursor samples, indicating that the particles contained disorderly arranged elements without a crystalline nature. On the other hand, the calcined samples exhibited a cubic structure with improved crystallinity. Charge transfer between the Eu^{3+} and O^{2-} ions increases with increasing crystallite size of the particle.[1] Therefore, at higher calcination temperature the samples showed intense CTB and considerable f-f transitions. The f-f transitions of Eu^{3+} ions appeared in the near-ultraviolet (NUV) (393 nm) and UV (465 and 533 nm) regions, which are suitable for bio-

imaging applications.

The PL emission spectra revealed a strong emission band between 602 and 635 nm with a band maximum at 610 nm due to the forced electric-dipole (hypersensitive) ($^5D_0 \rightarrow {}^7F_2$) transition, as well as weak emission bands between 585 and 601 nm corresponding to the magnetic-dipole ($^5D_0 \rightarrow {}^7F_1$) transition. Similarly, the additional emission bands 579, 649, and 705 nm are caused by the ($^5D_0 \rightarrow {}^7F_0$), ($^5D_0 \rightarrow {}^7F_3$), and ($^5D_0 \rightarrow {}^7F_4$) transitions of Eu^{3+} ions, respectively. The resulting PL emission spectra clearly exhibited an intense hypersensitive transition compared to that of a magnetic dipole transition for all samples indicating that Eu^{3+} ions have C_2 site symmetry. In a cubic Gd_2O_3 lattice, the unit cell consists of two distinct cation sites with point symmetry groups C_2 and S_6 (or C_{3i}) at a ratio of 3:1 (i.e., 24 cation sites having C_2 symmetry and 8 sites with S_6 symmetry); both sites consist of octahedral coordination [2]. The resulting emission spectra clarified that most of Eu^{3+} ions occupied the C_2 symmetry compared to S_6 symmetry. As a result, an intense hypersensitive transition was achieved. The magnetic dipole transition will dominate the electric dipole transition if most of the Eu^{3+} ions occupy the S_6 site symmetry of Gd^{3+} ions. In addition, the ratio between the integrated intensities of these two transitions shows the asymmetric nature around the Eu^{3+} ions in the host lattice.[3] Generally, the ^7F_J energy levels of Eu^{3+} ions are split into some components under the crystal field effects caused by the surrounding ions. Under C_2 site symmetry, the $^7F_1$ and $^7F_2$ energy levels of the calcined samples are split into three sublevels due to the completely elevated *"2J+1"* degeneracy of the ground state Eu^{3+}, whereas there was no considerable splitting observed for the amorphous samples. The PL emission spectra of calcined samples showed that, the $^7F_1$ level is split into three stark sublevels peaking at 587, 591, and 597 nm. Similarly, the $^7F_2$ energy level is also split into three components and the spectral positions of

the peaks were 610, 620 and 627. The PL results suggests that the GdC@mSi and Gd@mSi samples are suitable for bio-imaging applications.

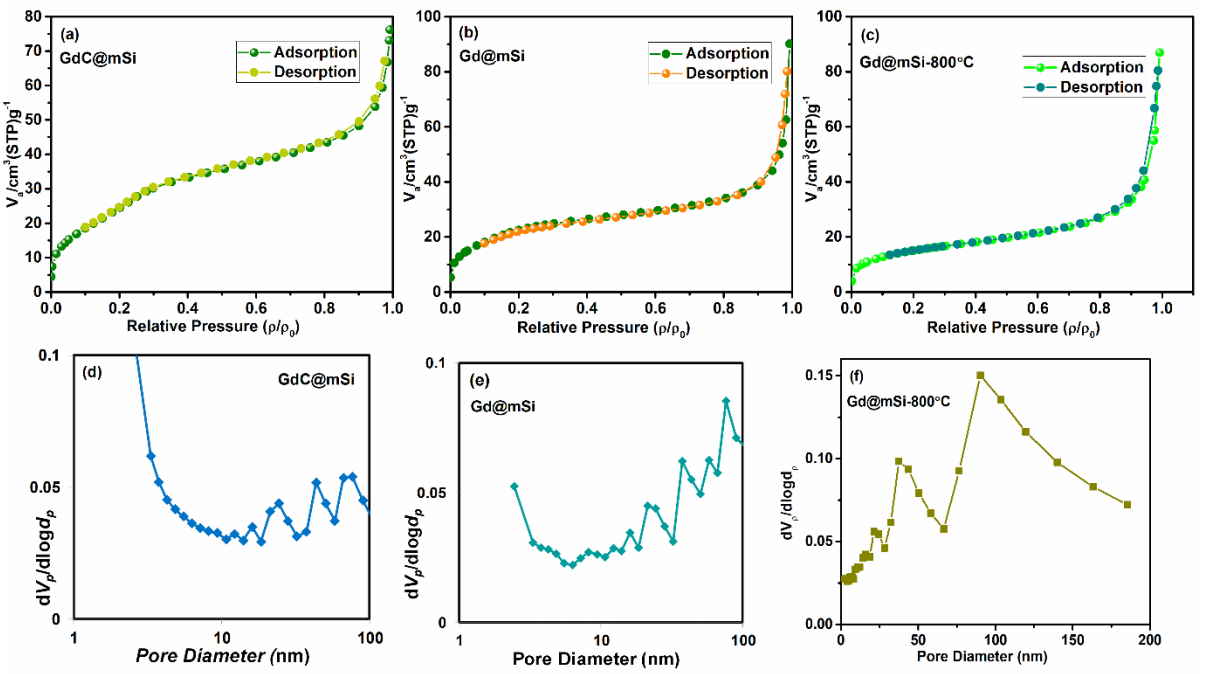

Fig. S3 BET surface area of (a) GdC@mSi (b) Gd@mSi, and (c) Gd@mSi-800 ºC CSNPs and BJH pore size distribution plots of (d) GdC@mSi, (e) Gd@mSi, and (f) Gd@mSi-800 ºC CSNPs.

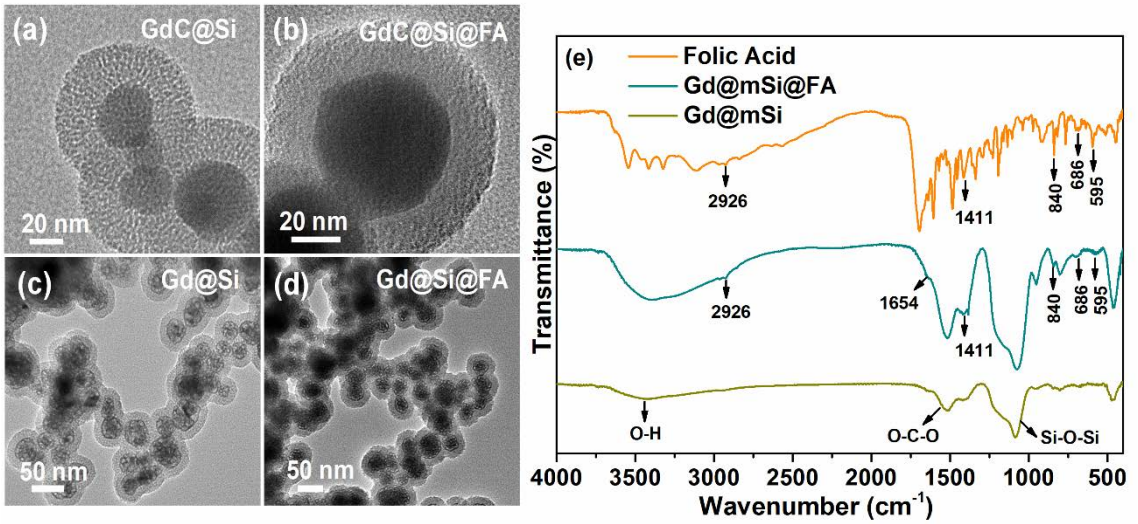

Fig. S4 Comparison between the FE-TEM images of GdC@mSi and Gd@mSi CSNPs before (a & c) and after (b & d) FA coating, respectively and (e) FTIR spectra of Gd@mSi core-shell nanoparticles before and after FA coating

Fig. S4e shows the FTIR spectra of Gd@mSi core-shell nanoparticles before and after FA coating and compared with folic acid spectrum. From the spectra, the O-H stretching band was observed at 3404 cm^{-1} and the characteristic band of O-C-O was detected at 1510 cm^{-1} region.[4] Likewise, the characteristic band of silica (Si-O) observed at 1084 cm^{-1} region confirmed the presence of mesoporous silica in Gd@mSi samples. The characteristic peaks of folic acid was observed at 2926, 1654, 1411, 840,686, and 595 cm^{-1} region where the absorption band at 1654 cm^{-1} belongs to -$CONH_2$ group and the band at 1411 cm-1 corresponds to OH deformation band of phenyl skeleton of folic acid.[5] Furthermore, the bands at 3544, 3416, 3320 and 3113 cm-1 were combined with O-H stretching bands; as a result, the broad ness of the O-H band was increased after folic acid conjugation as compared to Gd@mSi sample.

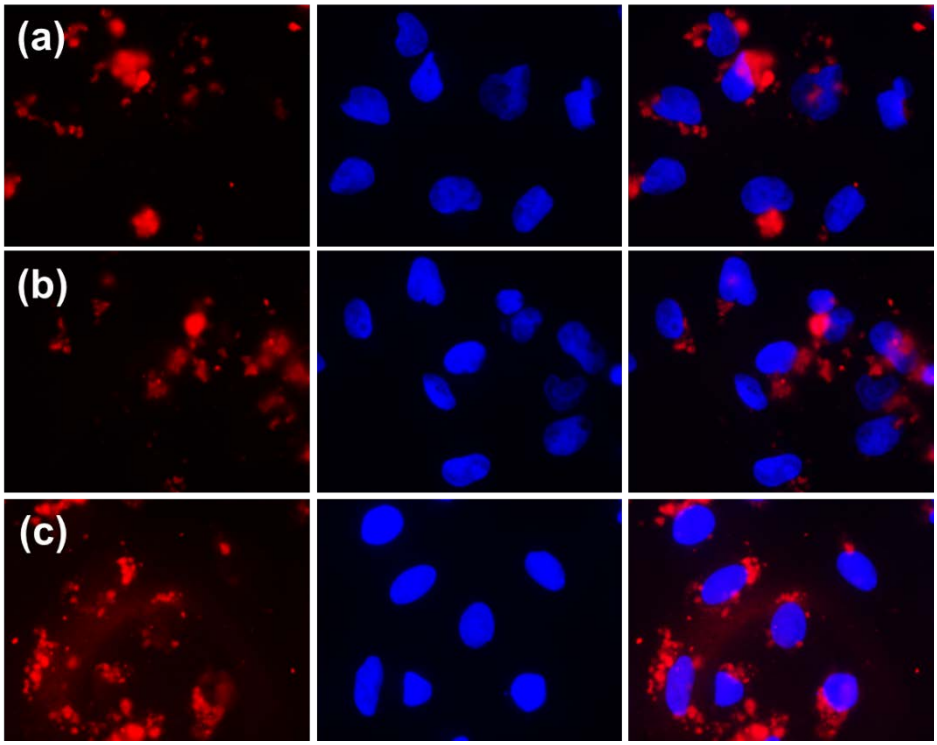

Fig. S5 (a-c) confocal imaging of Gd@mSi CSNPs (calcined at 300, 400, and 500 °C, respectively) uptake by U2OS cancer cell lines: GdC@mSi and Gd@mSi CSNPs showing red-fluorescence images from the U2OS cell line, U2OS cell nucleus stained with DAPI, which exhibited blue color, and merged fluorescence images from the U2OS cell line, respectively.

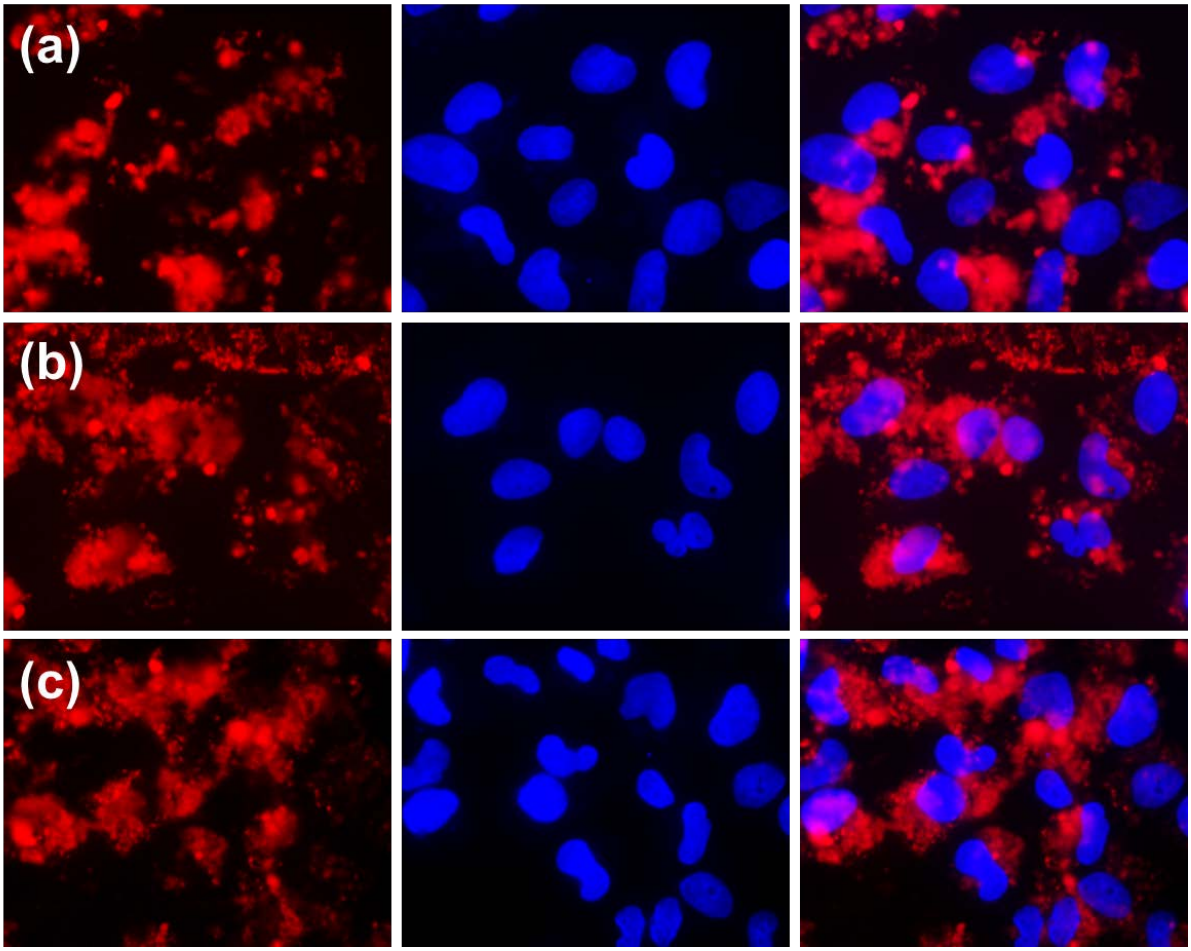

Fig. S6 (a-c) confocal imaging of Gd@mSi@FA CSNPs (calcined at 300, 400, and 500 °C, respectively) uptake by U2OS cancer cell lines.

References:

1. G. Seeta Rama Raju, E. Pavitra, G. Nagaraju and J. S. Yu, *Dalton trans.*, 2015, **44**, 1790-1799.
2. M. L. Debasu, D. Ananias, A. G. Macedo, J. Rocha and L. D. Carlos, *J. Phys. Chem. C*, 2011, **115**, 15297-15303.
3. E. Pavitra, G. Seeta Rama Raju, J. Y. Park, Y. H. Ko and J. S. Yu, *J. Alloys Compd.*, 2013, **553**, 291-298.
4. G. S. R. Raju, E. Pavitra and J. S. Yu, *Dalton trans.*, 2013, **42**, 11400-11410.
5. Q. Yuan, S. Hein and R. D. K. Misra, *Acta Biomaterialia*, 2010, **6**, 2732-2739.